Inverse Scattering Study

report on the OTKA Project Nr T047035

performed at TU Budapest between 2004-2008

Principal Investigator:
Barnabas Apagyi, Department of Theoretical Physics, Budapest University of Technology and Economics, Budapest

Participants:

Miklos Horvath, Department of Mathematics, Budapest University of Technology and Economics, Budapest

Daniel Schumayer, Department of Physics, Otago University, Dunedin, New Zealand

Peter Levay, Department of Theoretical Physics, Budapest University of Technology and Economics, Budapest

1. Aims

The research proposal is grown up from our intensive work and experience in the research on the quantum mechanical inverse scattering problem. Immense scientific efforts are and were made in Bose-Einstein-Condensation (BEC) in order to gain new knowledge and deeper insight in the properties and the forming of observable BE condensates. The stability of these condensates depends on the interaction between the atoms forming the condensates.
The first main aim of our research project was the exploration of stable solutions for two-component BE condensates by considering the general region of stable solutions of coupled Gross-Pitaevskii equations describing the two component BE condensates. For the solution of these equations an inverse scattering problem has to be solved with coupled reaction channels. The second main aim was directly connected to this problem. We planned to develop new practical methods of the solution of the inverse scattering problem at fixed energy for coupled reaction channels. Whereas the elastic inverse scattering problem at fixed energy can be solved with several known methods giving complex potentials from the elastic phase shifts, the three-dimensional coupled inverse problem at fixed energy is less studied and lacks for such methods. We wanted to investigate this basic question by searching for solutions within a Born-like approximation and within the algebraic scattering theory. Both methods should be used for obtaining potentials and couplings from S-matrices connected with experimental elastic and reaction cross sections.
Both aims are and were actual and basic for our understanding of interactions between

atoms, ions or nuclei. They should lead to important results which should be published in internationally recognized journals like our former work in the fields of Bose-Einstein-Condensates and of Inverse Scattering Problems.

2. Summary

The inverse quantum mechanical scattering problem at fixed scattering energy searches for the elastic potential or coupling potentials from a set of phase shifts or from a S-matrix. The phase shifts as a function of the angular momentum can be obtained from measured differential cross sections at fixed energy. To solve the inverse scattering problem is a very difficult mathematical question. Here, we do not discuss the uniqueness of the different methods, to extract potentials from the phase shifts.

During the project we developed the inverse method of Cox and Thompson for applications, simplified the solution method and applied this method to get the effective Rb-Rb interatomic potential from ultracold Bose gas collisions ($T < 1$ μK). We worked out a new solution method of the inverse scattering problem at a fixed energy for a potential which is zero beyond a fixed radius. Further we gave a first solution of the inverse scattering problem for coupled channels at a fixed energy. This solution is based on the Born approximation and allows to analyze coupled channel problems with the corresponding S-matrix. We investigated the stability of static solitonic excitations occuring in Bose-Einstein condensates.

With the Cox-Thompson method it is possible to invert phase shifts to potentials which are finite at the coordinate origin and have a first momentum $\int V(r)rdr$ which can be different from zero. The Cox-Thompson method leads to highly nonlinear equations. We found numerical solutions from phase shifts of complex potentials and partly analytical solutions in the case that only phase shifts contribute which belong to even or odd angular momenta. The latter point is important and gives a great simplification for problems of the elastic scattering of bosons (even angular momenta) or fermions (odd angular momenta). We showed that this latter method can also be approximately applied in various variants. We applied the Cox-Thompson method for the scattering of ^{87}Rb on ^{87}Rb at very low energies, where these atoms form a Bose-Einstein condensate. We obtained an energy-dependent potential which changes its characteristic from repulsion to attraction near the $\ell = 2$ resonance at $T \approx 275$ μK.

The complicated inversion problem for coupled channels was solved for cases where the Born approximation is justified. We have up to now only inverted S-matrices from known given potentials. This method has the great advantage that one needs only S-matrix elements, which relate the elastic channel with the inelastic channels, and one obtains the coupling potentials between the elastic and inelastic channels directly. This procedure is waiting for applications with measured S-matrices where we would find realistic coupling potentials which can be compared with coupling potentials calculated with model assumptions.

In this project we worked out a treatment for the stability of an atomic two-component Bose-Einstein condensate. We considered the macroscopic dynamics in such a condensate by two coupled nonlinear Schrödinger equations, known as Gross-Pitaevskii equations. Depending on the interspecies scattering length we got information about the

two-component system which may show solitonic features. We applied the formalism to a two-component Bose-Einstein condensate consisting of a mixture ^{7}Li - ^{87}Rb.
The project gave new, internationally recognized developments in the mathematical theory of the solution of the inverse scattering problem at fixed energy. Also new knowledge in the field of Bose-Einstein condensates was gained.

3. Report on the main results

3.1 Extension of the inverse method of Cox and Thompson to complex potentials and experimental data

Phase shifts obtained at fixed energies are usually used together with the modified Newton-Sabatier method to construct the underlying potential. However this method yields local potentials which are infinite at the origin and which have a vanishing first momentum $\int V(r) r dr = 0$. Both disadvantages of the Newton-Sabatier method are avoided by the Cox-Thompson method developed here for practical applications first by B. Apagyi, Z. Harman and W. Scheid (J. Phys. A: Math. Gen. **36** (2003) 4815). We have extended this method to complex potentials and experimental data. In chapter 3.2 we describe a recent extension to fermionic and bosonic scattering wave functions which simplifies this method to a large extent.
Cox and Thompson started with a Povzner-Levitan-representation for the regular scattering wave function

$$\phi_l(r) = u_l(r) - \int_0^r \mathrm{d}r'\, r'^{-2} K(r,r') u_l(r'), \tag{1}$$

where $\phi_l(r)$ has to fulfill the Schrödinger equation with the searched potential. (We use dimensionless units and k is fixed at 1 so that $kr => r$, $\frac{2\mu}{\hbar^2 k^2} U(r) = V(r)$, $\frac{2\mu}{\hbar^2 k^2} E = 1$.) Using the operators

$$D(r) = D_0(r) - r^2 V(r), \quad D_0(r) = r^2 \left(\frac{\partial^2}{\partial r^2} + 1 \right), \tag{2}$$

the Schrödinger equation can be written in the form

$$D(r)\phi_l(r) = l(l+1)\phi_l(r). \tag{3}$$

The function $u_l(r)$ is the regular solution of the corresponding Schrödinger equation without a potential

$$D_0(r) u_l(r) = l(l+1) u_l(r). \tag{4}$$

Inserting $\phi_l(r)$ into the Schrödinger equation and assuming that the kernel $K(r,r')$ fulfills the partial differential equation

$$D(r)K(r,r') = D_0(r')K(r,r'),$$

one obtains the potentials as

$$V(r) = -\frac{2}{r}\frac{d}{dr}\left(\frac{K(r,r)}{r}\right).$$

The transformation kernel $K(r,r')$ can be written as

$$K(r,r') = \sum_{L\in T} A_L(r) u_L(r'),$$

where the indices $L \in T$ are taken from a set T of generalized shifted angular momentum quantum numbers being disjunct with the set $\{l\} \equiv S$ of real integer physical angular momenta ($S \cap T = \{\}$). The functions $A_L(r)$ can be determined by starting with the Gel'fand-Levitan-Marchenko–type integral equation for the transformation kernel

$$K(r,r') = g(r,r') - \int_0^r \mathrm{d}r'' r''^{-2} K(r,r'') g(r'',r'), \qquad r \geq r'$$

and then applying the Cox-Thompson ansatz for the symmetric kernel

$$g(r,r') = \sum_{l\in S} \gamma_l u_l(r_<) v_l(r_>) = g(r,r'),$$

where $r_<(r_>)$ stands for the minimum (maximum) of the variables r, r', v_l are irregular Neumann functions satisfying equation (4) with the behaviour r^{-l} at the origin, and γ_l denotes expansion coefficients. From the above equations one obtains a system of linear equations for the functions $A_L(r)$:

$$\sum_{L\in T} A_L(r) \frac{u_L(r) \times dv_l(r)/dr - du_L(r)/dr \times v_l(r)}{l(l+1) - L(L+1)} = v_l(r), \qquad l \in S,$$

where the set T is as yet unknow. Another system of equations can be obtained for the coefficients γ_l:

$$\sum_{l\in S} \frac{\gamma_l}{l(l+1) - L(L+1)} = 1, \qquad L \in T,$$

which has the solution

$$\gamma_l = \frac{\prod_{L\in T}[l(l+1) - L(L+1)]}{\prod_{l'\in S, l'\neq l}[l(l+1) - l'(l'+1)]}, \quad l \in S.$$

Connecting the coefficients $A_L(r)$ with the physical phases we calculated finally the equations

$$S_l = \frac{1 + i\mathcal{K}_l^+}{1 - i\mathcal{K}_l^-}, \qquad l \in S$$

with the scattering matrix elements $S_l = \exp(2i\delta_l)$ and the quantities $\mathcal{K}_l^\pm$ defined as

$$\mathcal{K}_l^\pm = \sum_{L\in T, l'\in S} (M_{\sin})_{lL} (M_{\cos}^{-1})_{Ll'} e^{\pm i(l-l')\pi/2}, \qquad l \in S,$$

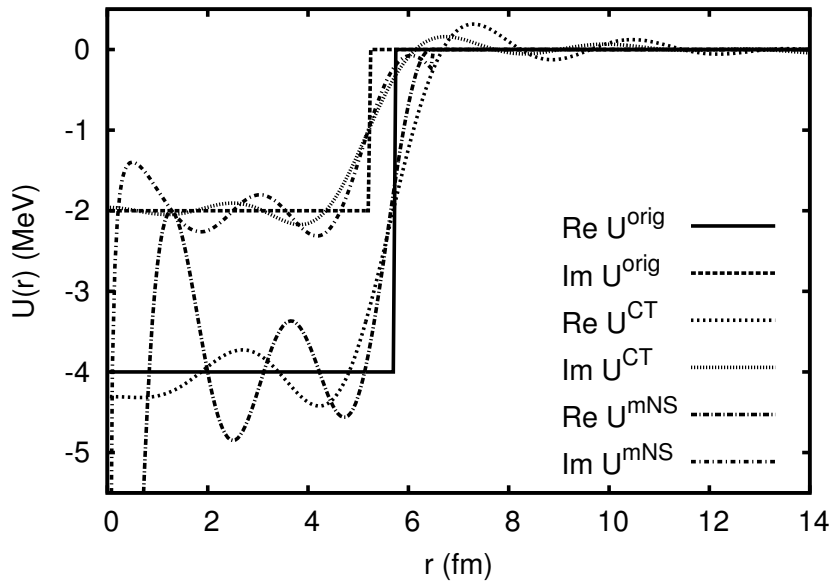

Figure 1: Complex box potential: Results for the inversion of 11 phase shifts at $E_{cm} = 22$ MeV using the CT- and mNS-method. The masses of the scattered particles were chosen as $M_1 = M$ and $M_2 = 20 \cdot M$, where M is the nucleon mass.

where the square matrices are defined by

$$\left\{ \begin{array}{c} M_{\sin} \\ M_{\cos} \end{array} \right\}_{lL} = \frac{1}{L(L+1) - l(l+1)} \left\{ \begin{array}{c} \sin\left((l-L)\frac{\pi}{2}\right) \\ \cos\left((l-L)\frac{\pi}{2}\right) \end{array} \right\}, \qquad l \in S,\, L \in T,\, S \cap T = \{\,\}.$$

The numerical search for complex $L-$values from complex phase shifts is mathematically very complex and needs advanced numerical methods like the Newton-Raphson or simulated annealing methods.
The application of inversion methods has two sources of errors, namely the quality of the phase shifts of the measured differential cross section and the quality of the inversion method from the phase shifts to the potential. First we will concentrate our discussion on the second source of errors. In Figs. 1 and 2 we demonstrate potentials gained with phases from given potentials with the Cox-Thompson (CT) and the modified Newton-Sabatier (mNS) methods. One recognizes the advantage of the CT method. The inversion leads to a finite value of the potential at the origin.
The amplitude of the oscillations of the inverted potentials depends on the maximum angular momentum l_{max}, on the precision of phase shifts and of the calculation. It is very difficult the formulate precise error formulas in an analytical form since the Newton-Sabatier and the Cox-Thompson method are highly nonlinear theories. Such mathematical investigations on the stability and precision of the CT-method are really needed for future advance of this ill-conditioned inversion problem and should be planned in a new proposal of investigations to the inverse scattering problem.
As an example for phase shifts related to experimental scattering data we considered the elastic $n - \alpha$ scattering below the inelastic threshold $n + \alpha \rightarrow d + t$ at $E_\alpha = 22.06$ MeV. Since the CT-method assumes a local central potential, we simplified the actual problem

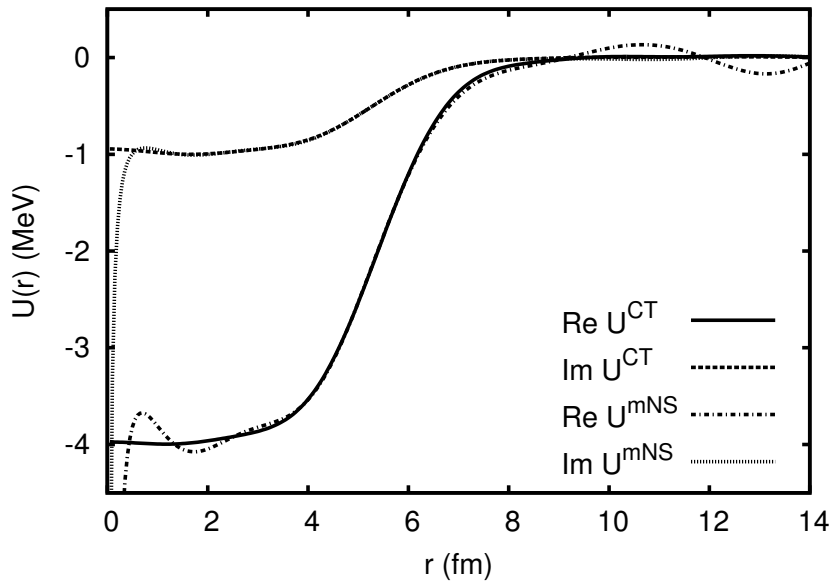

Figure 2: Complex Woods-Saxon potential: Results for the inversion of 14 phase shifts at $E_{cm} = 25$ MeV using the CT- and mNS-method. The masses of the scattered particles were chosen as $M_1 = M$ and $M_2 = 20 \cdot M$, where M is the nucleon mass. Because of the good agreement of the CT inversion potential with the original Woods-Saxon-potential, the latter one is not shown in the figure.

considerably. We partly neglected the spin-orbit potential and used complex-valued phase shifts. Also phase shifts were derived by Chen and Tornow from experimental differential cross section data for the scattering of neutrons on ^{12}C. We used the phase shifts for inversion. In Fig. 3. we show real and imaginary central potentials obtained by the CT-inversion from these phase shifts. We conclude from the results obtained for the $n-$nucleus scattering that the CT inverse method deserves to be extended further to be able to treat phase shift data originated from charged particle collisions.

3.2 Simplified solution of the Cox-Thompson inverse scattering method at fixed energy

The Cox-Thompson method connects the $S-$matrix with a "reactance" matrix $\mathcal{K}_l^{\pm}$ (see Section 3.1)(T. Palmai, H. Horvath, B. Apagyi, J. Phys. A: Math. Theor. **41** (2008) 235305)

$$S_l = \frac{1 + i\mathcal{K}_l^+}{1 - i\mathcal{K}_l^-}, \qquad l \in S, \tag{5}$$

where

$$\mathcal{K}_l^{\pm} = \sum_{L \in T, l' \in S} (M_{\sin})_{lL} (M_{\cos}^{-1})_{Ll'} e^{\pm i(l-l')\pi/2}, \qquad l \in S,$$

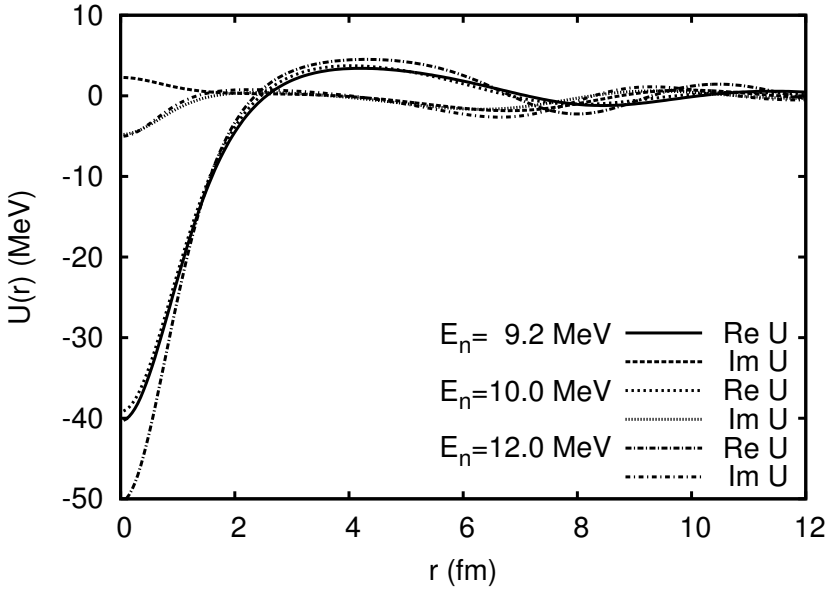

Figure 3: Real and imaginary central potentials inverted from phase shifts of $n-{}^{12}$C differential cross sections at the neutron energies $E_n^{\rm lab}=$ 9.2, 10 and 12 MeV.

and

$$\left\{ \begin{array}{c} M_{\rm sin} \\ M_{\rm cos} \end{array} \right\}_{lL} = \frac{1}{L(L+1)-l(l+1)} \left\{ \begin{array}{c} \sin\left((l-L)\frac{\pi}{2}\right) \\ \cos\left((l-L)\frac{\pi}{2}\right) \end{array} \right\}, \qquad l\in S,\, L\in T,\, S\cap T=\{\,\}.$$

An essential simplification has been found which can be used in the cases when only even or odd partial waves contribute to the scattering. This simplifications of the equations can be used to construct different simple approximations to the Cox-Thompson-method. For example, in the scattering of ^{12}C on ^{12}C the elastic cross sections are generated by even partial phase shifts only.
By solving the Gel'fand-Levitan-Marchenko–type integral equation one writes the transformation kernel in the form as a sum over an artificial angular momentum space $L\in T$:

$$K(x,y)=\sum_{L\in T} A_L(x)u_L(y).$$

One finds for the asymptotic expansion functions $A_L^{\rm a}(x)\equiv A_L(x\to\infty)$ the relation

$$\sum_{L\in T} A_L^{\rm a}(x)\frac{\cos((l-L)\frac{\pi}{2})}{l(l+1)-L(L+1)} = -\cos(x-l\frac{\pi}{2}), \qquad l\in S.$$

If this equation is differentiated twice with respect to x, we obtained the following equation

$$\frac{d^2A_L^{\rm a}(x)}{dx^2}=-A_L^{\rm a}(x),$$

which has a periodic solution

$$A_L^{\rm a}(x)=a_L\cos(x)+b_L\sin(x).$$

Then we introduced two systems of equations for even $l = l_e$ and odd $l = l_o$ angular momenta as follows

$$\sum_{L\in T_{\rm e}} \left\{ \begin{array}{c} a_L \\ b_L \end{array} \right\} \frac{\cos\left((l-L)\frac{\pi}{2}\right)}{L(L+1)-l(l+1)} = \left\{ \begin{array}{c} \cos\left(l\frac{\pi}{2}\right) \\ \sin\left(l\frac{\pi}{2}\right) \end{array} \right\}, \qquad l \in S_{\rm e}$$

and

$$\sum_{L\in T_{\rm o}} \left\{ \begin{array}{c} a_L \\ b_L \end{array} \right\} \frac{\cos\left((l-L)\frac{\pi}{2}\right)}{L(L+1)-l(l+1)} = \left\{ \begin{array}{c} \cos\left(l\frac{\pi}{2}\right) \\ \sin\left(l\frac{\pi}{2}\right) \end{array} \right\}, \qquad l \in S_{\rm o},$$

where $|T_{\rm e}| = |S_{\rm e}|$, $|T_{\rm o}| = |S_{\rm o}|$ and $T_{\rm e} \cap S_{\rm e} = \emptyset$, $T_{\rm o} \cap S_{\rm o} = \emptyset$. These systems can be analytically solved. For even l value we obtained

$$a_L = \frac{\prod_{l\in S_{\rm e}}(L(L+1)-l(l+1))}{\prod_{L'\in T_{\rm e}\setminus\{L\}}(L(L+1)-L'(L'+1))}\frac{1}{\cos\left(L\frac{\pi}{2}\right)}, \qquad b_L = 0, \qquad L \in T_{\rm e},$$

and similarly for odd orbital angular momenta $l_o \in S_o$. Now by using these analytical expressions one obtains the final solution to the CT method for even l as:

$$\tan(\delta_l) = -\sum_{L\in T_{\rm e}} \frac{\prod_{l'\in S_{\rm e}\setminus\{l\}}(L(L+1)-l'(l'+1))}{\prod_{L'\in T_{\rm e}\setminus\{L\}}(L(L+1)-L'(L'+1))} \tan\left(L\frac{\pi}{2}\right), \qquad l \in S_{\rm e}. \qquad (6)$$

A similar relation is obtained for odd orbital angular momenta $l_o \in S_o$.
The above equations determine the unknown set T_e of shifted angular momenta L. These equations are much simpler as the above equations which contain the inversion of the matrix of M_{cos} involving the unknowns of shifted angular momenta L. The above equations are presumably easier to be solved for the set T_e (or T_o) if the input phase shifts are given. We showed that the solutions with even $l = l_e$ of equations (6) are equivalent to the solution of equation (5).
There are several approximations possible with this simplified method. One can solve the inverse potential for the sets T_e and T_o and obtains the potentials q_e and q_o. One can simply add them together to get the approximation of the interaction potential $q_A(x) = q_e(x) + q_o(x)$. This is called the potential approximation A. One may try to approximate the set of the shifted angular momenta themselves by solving the equations for even and odd phase shifts separately, obtaining the sets T_e and T_o (approximation T). One gets the $T-$set approximation $T_a = T_e \cup T_o$ and then the approximate potential $q_T(x)$. If the collision is dominated by a single partial wave as in the case of resonance scattering then the equations can be solved for $N = 1$, and this results in the simple expression $L = l - 2\delta_l/\pi$ for the shifted angular momentum (approximation L). This approximation used for all shifted angular momenta yields an inverted potential denoted by $q_L(x)$.
We applied the new method to calculate an effective ^{87}Rb+^{87}Rb-potential observed in ultracold Bose-gas collision at an energy of $E = 303\mu$K. The inverse calculation uses only even measured phase shifts with angular momenta $l = 0, 2, 4$, respectively. The resulting potential shown in Fig. 4 is identical with the potential obtained by solving the complete set of equations (see chapter 3.3).
We calculated also the inverse potential for the n+^{12}C scattering at $E_{lab} = 10$ MeV with complex-value phase shifts derived by Chen and Thornow from experimental cross

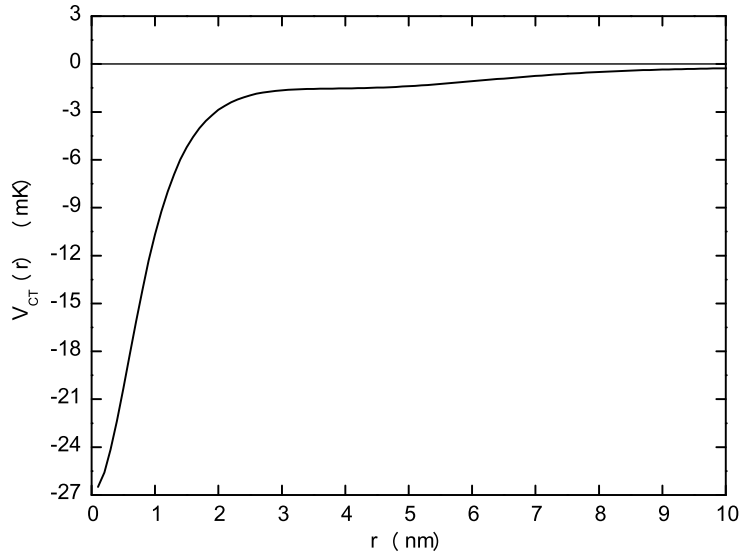

Figure 4: Effective ^{87}Rb+^{87}Rb inverse potential $V_{\rm CT}$ (in mK) as a function of the radial distance r (in nm) at an energy $E_{cm} = 303\,\mu$K.

sections. The inverse potentials are obtained with different approximations. It is assumed that the potential calculated by the original CT-method would be the best one. In Fig. 5 we show inverse potentials obtained with the approximations A,T, and L.
The range of applicability of the new formulas is wider than the original Cox-Thompson method. We have demonstrated the applicability of the new equations which make the solution of the CT inverse scattering method at fixed energy much easier.

3.3 The effective Rb-Rb interatomic potential from ultracold Bose-gas collisions

At very low energies, at the end of the energy scale, one can cool down atoms to the ultracold regime ($< 1\,\mu$K), to form a Bose-Einstein condensate and explore the low-energy properties of the atomic interaction. At these temperatures collisions play a major role in affecting the static and dynamic properties of the condensate, e.g. stability, lifetime, and thermalization rate. In this regime inelastic processes are usually negligible. Here, we contributed to characterize or even to reconstruct an effective inter-atomic potential from scattering phase shifts by using the inverse scattering method by assuming that there exists an effective spherically symmetric potential which is the cause of the observed scattering events (D. Schumayer, O. Melchert, W. Scheid, B. Apagyi, J. Phys. B: At. Mol. Opt. Phys. **41** (2008) 035302).
We employed the fixed energy inverse scattering method of Cox and Thompson (CT) in order to derive model-independent potentials from given phase shifts resulting from

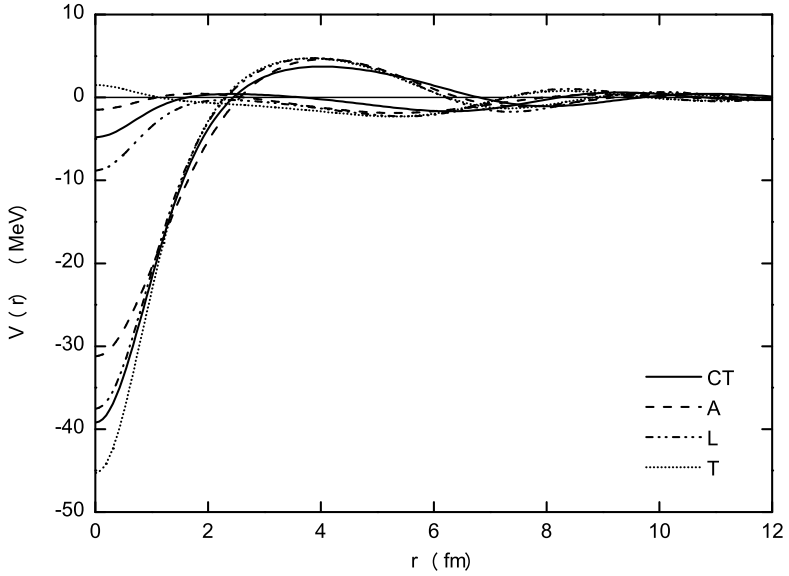

Figure 5: Inverse potentials obtained from input phase shifts up to $l = 4$ for n scattering on ^{12}C at an energy $E_{\rm n}^{\rm lab} = 10$ MeV ($E_{\rm n}^{\rm c.m} = 9.23$ MeV, $k = 0.638$ fm^{-1}). Curves obtained by the CT and by the approximate methods are labeled according to the procedure discussed in the text.

experiments with a Rb-Bose gas in traps. The CT method leads to a system of nonlinear equations

$$\exp\left(2i\delta_l\right) = \frac{1 + i\mathcal{K}_l^+}{1 - i\mathcal{K}_l^-},$$

where the reactance matrix is defined as

$$\mathcal{K}_l^{\pm} = \sum_{L\in T, l'\in S} \mathcal{N}_{lL} \left(\mathcal{M}^{-1}\right)_{Ll'} e^{\pm i(l-l')\pi/2}, \quad l \in S$$

with the square matrices

$$\left\{ \begin{array}{c} \mathcal{N} \\ \mathcal{M} \end{array} \right\}_{lL} = \frac{1}{L(L+1) - l(l+1)} \left\{ \begin{array}{c} \sin\left((l-L)\pi/2\right) \\ \cos\left((l-L)\pi/2\right) \end{array} \right\}, \quad l \in S, L \in T, S \cap T = \{\,\},$$

containing the unknown $L-$values. Once the set T is determined by solving the highly nonlinear equation given above for L, we calculate coefficient functions $A_L(r)$ using the system of linear equations

$$\sum_{L\in T} A_L(r)(j_L(r) \times n_l'(r) - j_L'(r) \times n_l(r))/[l(l+1) - L(L+1)] = n_l(r),$$

where j_L and n_l denote spherical Bessel and Neumann functions. Next, we calculate the

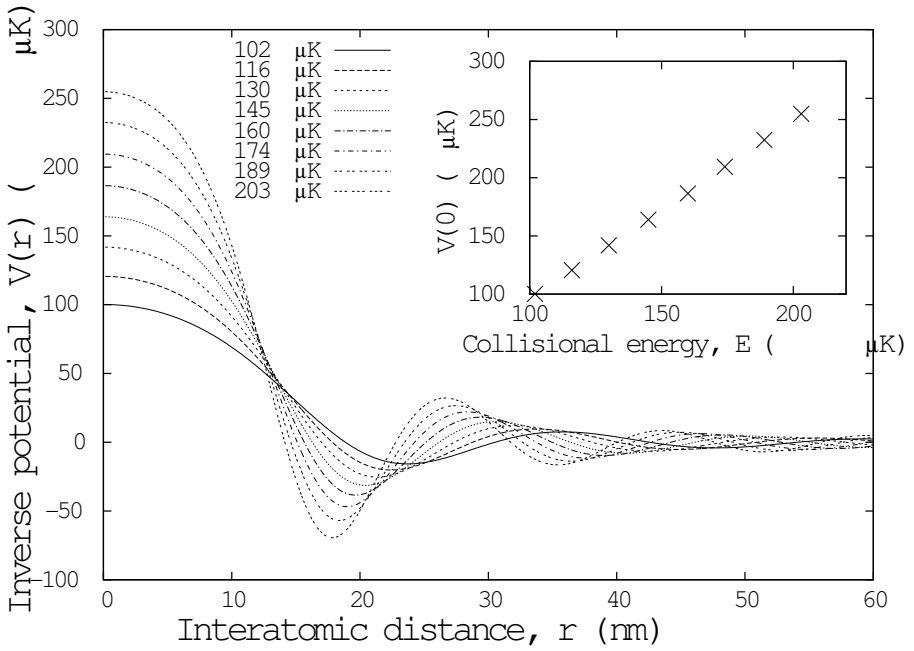

Figure 6: Inverse potentials from the $l = 0, 2, 4$ experimental phase shifts at energies E=102-203 μK below the $d-$resonance. The inset shows the central amplitude of the inverse potential as a function of collision energy.

potential with the expansion coefficients $A_L(r)$

$$V(r) = -\frac{2}{r}\frac{d}{dr}\sum_{L\in T} A_L(r) j_l(r)/r.$$

In Fig. 6 we present the inversion potentials for the energy range between 100 and 200 μK which lie below the characteristic $l = 2$ resonance of ^{87}Rb-^{87}Rb scattering at ~ 275 μK. The inversion potentials reproduce the input phase shifts well within the considered energy region as demonstrated in Fig. 7 where both input and output phase shifts are shown. Fig. 8 gives the inversion potentials from 200 to 400 μK. There occurs an abrupt change of potential strength $V(0)$ at $r = 0$ from repulsion to attraction when the collision energy crosses the $l = 2$ resonance at $\sim 275\,\mu$K.
Since the input data stem entirely from experimentally confirmed data we expected that the sudden change of the inner strength of the potential should be observed in future Bose-gas experiments. This inversion technique is useful if high-resolution data are available, the corresponding potential has not already been studied with models and if one needs an intuitive picture about the interaction in a given energy range.

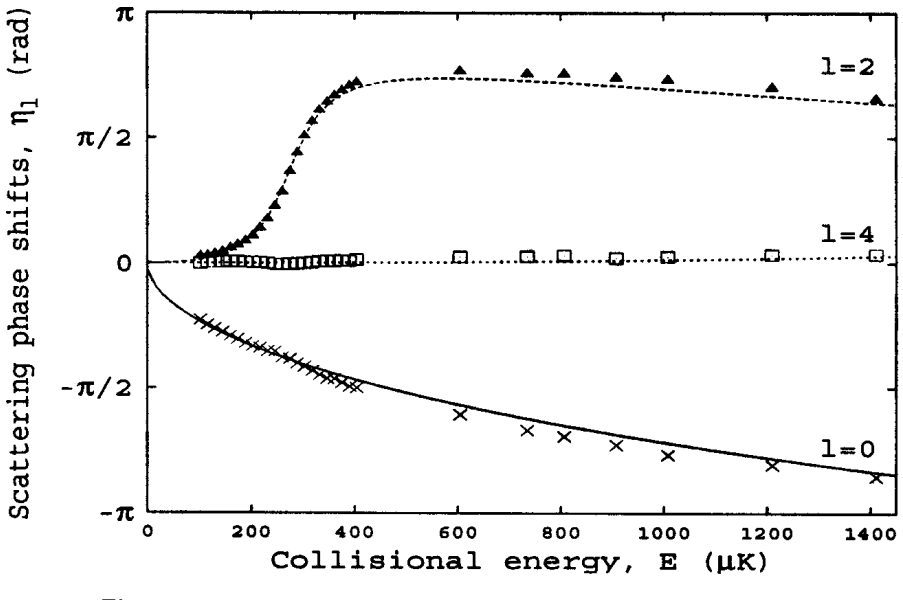

Figure 7: Phase shifts of the first three allowed partial waves with $l = 0, 2, 4$. Solid and dashed lines represent the original input data. The symbols stand for phase shifts calculated from the inverse potentials shown in Figs 6 and 8.

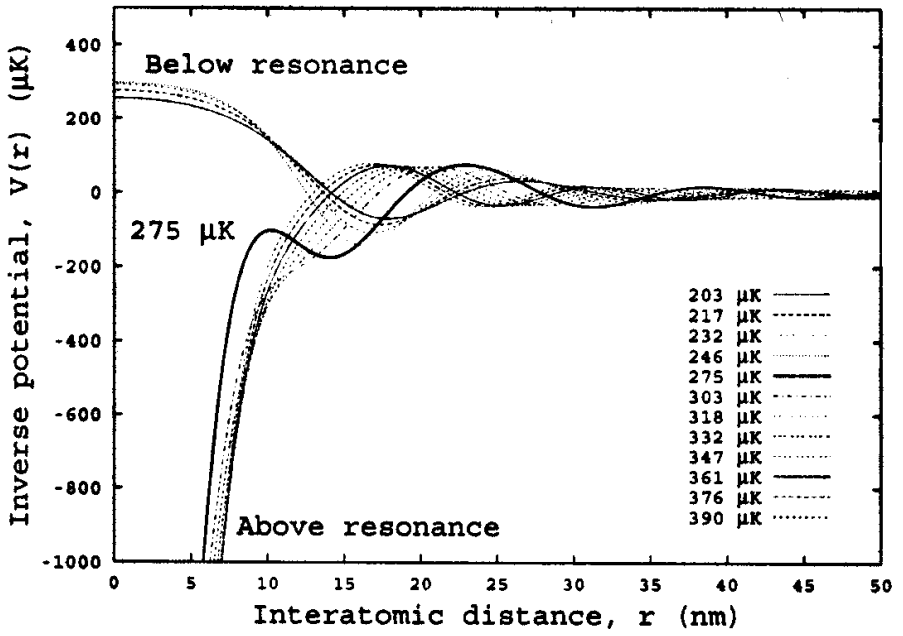

Figure 8: Inverse potentials obtained from the experimental $l = 0, 2, 4$ scattering phase shifts around the $d-$resonance at $\sim 275\,\mu$K.

3.4 New solution of the inverse scattering problem at fixed energy for a potential which is zero beyond a fixed radius.

We consider the radial Schödinger equation

$$-\varphi_l''(r) + \left(\frac{l(l+1)}{r^2} + q(r) - k^2\right)\varphi_l(r) = 0$$

with the boundary conditions $\varphi_l(r \to 0) \approx r^{l+1}$, and $\varphi_l(r \to \infty) \approx \sin(kr - l\pi/2 + \delta_l)$ with angular momentum quantum numbers $l = 0, 1, 2, ...$ The physical potential $V(r)$ is related to the above potential by the relation $q(r) = V(r)/(\hbar^2/2m)$ with m being the reduced mass. The potential $q(r)$ is zero beyond a certain radius: $q(r \geq a) = 0$, and the wave function can be written as

$$\varphi_l(r \geq a) = \sqrt{r}\left(J_{l+\frac{1}{2}}(kr) - \tan(\delta_l(k))Y_{l+\frac{1}{2}}(kr)\right),$$

where $J_{l+\frac{1}{2}}$ and $Y_{l+\frac{1}{2}}$ are regular and irregular Bessel functions. After performing the transformations

$$\varphi_l(r) = \sqrt{r}y_l(x), \quad r = a\exp(-x), \quad 0 \leq r \leq a,$$

we obtained the transformed Schrödinger equation

$$-y_l''(x) + Q(x)y_l(x) = -(l+1/2)^2\, y_l(x) \tag{7}$$

$$Q(x) = r^2(q(r) - k^2), \quad 0 \leq x \leq \infty.$$

The former equation is an eigenvalue equation on the half line with eigenvalues at $\lambda = -(l+\frac{1}{2})^2$. The initial slope of these eigenfunctions is known to be:

$$\frac{y_l'(0)}{y_l(0)} = a\frac{\varphi_l'(a)}{\varphi_l(a)} - \frac{1}{2} = -ka\frac{J_{l+1/2}'(ka) - \tan\delta_l Y_{l+1/2}'(ka)}{J_{l+1/2}(ka) - \tan\delta_l Y_{l+1/2}(ka)}.$$

Equation (7) can be considered as a Sturm-Liouville equation whose inverse problem is solved for a long time. The inverse spectral problem gives the spectral function, if $Q(x) \equiv 0$ and $Y_\lambda(x) = \cos\left(\sqrt{\lambda}x\right)$ in the form

$$\rho_0(\lambda) = \begin{cases} \frac{2}{\pi}\sqrt{\lambda}, & \lambda \geq 0, \\ 0, & \lambda < 0. \end{cases}$$

Our solution method is based on the observation that the moments μ_l of the input function, i.e.,

$$\mu_l \equiv \int_0^\infty F(x)\exp(-(l+\frac{1}{2})x)dx \tag{8}$$

with $F(x) = \int_{-\infty}^{\infty} \cos(\sqrt{\lambda}x)\ d\sigma(\lambda)$ and with $\sigma(\lambda) = \rho(\lambda) - \rho_0(\lambda)$, can be expressed as following

$$\mu_l = \frac{(l+\frac{1}{2})}{ka} \quad \frac{J_{l+1/2}(ka) - \tan\delta_l Y_{l+1/2}(ka)}{J'_{l+1/2}(ka) - \tan\delta_l Y'_{l+1/2}(ka)} - 1.$$

A symmetrical input kernel can be obtained from the definition of $F(x)$

$$F(x,t) = \int_{-\infty}^{\infty} \cos(\sqrt{\lambda}x)\cos(\sqrt{\lambda}t)\ d\sigma(\lambda) = \frac{1}{2}(F(x+t) + F(|x-t|)).$$

Knowing the input kernel one can determine the transformation kernel $K(x,t)$ by solving the Gelfand-Levitan-Marchenko (GLM) equation:

$$0 = F(x,t) + K(x,t) + \int_0^x K(x,s)F(s,t)ds, \qquad 0 \le t \le x.$$

The transformation kernel yields the transformed potential

$$Q(x) = 2\frac{d}{dx}K(x,x).$$

To determine the input function $F(x)$ from the given momenta we supposed that we have only one bound state at $\lambda = \lambda_0 < 0$ in $Q(x)$. Then we write

$$F(x) \approx c_0 e^{(1/2-2d)x} + \sum_{l=1}^{L} c_l e^{-(l-1)x}$$

and solve the above equation (8) by the minimum norm method. This method yields a system of linear equations which can be written in matrix form as

$$H(d)c = \mu$$

with the matrix elements

$$H_{ij}(d) = \int_0^1 dt\ t^{2d+i+j-1} = \frac{1}{i+j+2d}, \qquad i,j = 0,1,..,L.$$

The unknown singularity position d is determined from the condition

$$|\sum c_l| = min$$

which provides the bound state energy of the potential $Q(x)$ from the relation

$$d = \frac{1}{4} - \frac{1}{2}\sqrt{-\lambda_0}.$$

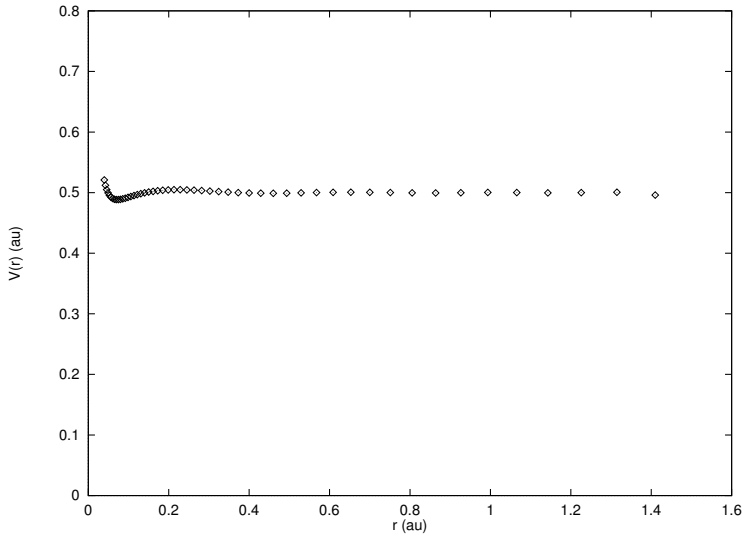

Figure 9: The inversion potential $V(r) = q(r)/2$ as a function of r. The results belong to the energy of $E_{cm} = 0.5$ a.u. ($k = 1$ a.u.).

By determining the expansion coefficients $c_0, c_1, ..., c_L$, and the bound state position λ_0 of $Q(x)$, one can finally derive the inverse potential $q(r)$. We applied this method to the box potential

$$V(r) = \begin{cases} 1/2 & \text{if} \quad 0 \leq r \leq a = \sqrt{2} \\ 0 & \text{else} \end{cases}$$

at the energy $E = 0.5$ a.u. with $k = 1$ a.u. We gained $\sqrt{-\lambda_0} = 0.3881$ for the bound state position in $Q(x)$. The Fig. 9 shows the potential inverted by phase shifts up to $l = 10$. The method is capable of reproducing the constant potential except for a narrow region at the origin where the breakdown is attributed to numerical imprecision of the extraction of the bound state value λ_0 of $Q(x)$ from the input phase shifts.
Another example is the Gauss potential of the form $V(r) = -2e^{-r^2/0.2}$. The results shown in Fig. 10 for the energy $E_{cm} = 1.125$ a.u. ($\hbar^2/m = 1$). We used eight phase shifts as input data and obtained $\sqrt{-\lambda_0} = 2.0853656$ for the bound state position in the potential $Q(x)$. The Gauss potential is well reproduced by this new method.

3.5 Coupled channel inverse scattering problem solution at fixed energy in Born approximation

We developed an approximation method based on the first Born approximation for the solution of the quantum inverse scattering problem at fixed energy for coupled reaction channels (S. Jesgarz, B. Apagyi, W. Scheid, J. Phys. A: Math. Gen. **37** (2004) 8721). This method gives us a local coupling matrix from the $S-$matrix.
We first formulated the Hamiltonian for the coupled channel problem

$$\hat{H}(\boldsymbol{r}, \xi) = \hat{T}(\boldsymbol{r}) + \hat{h}(\xi) + \hat{W}(\boldsymbol{r}, \xi).$$

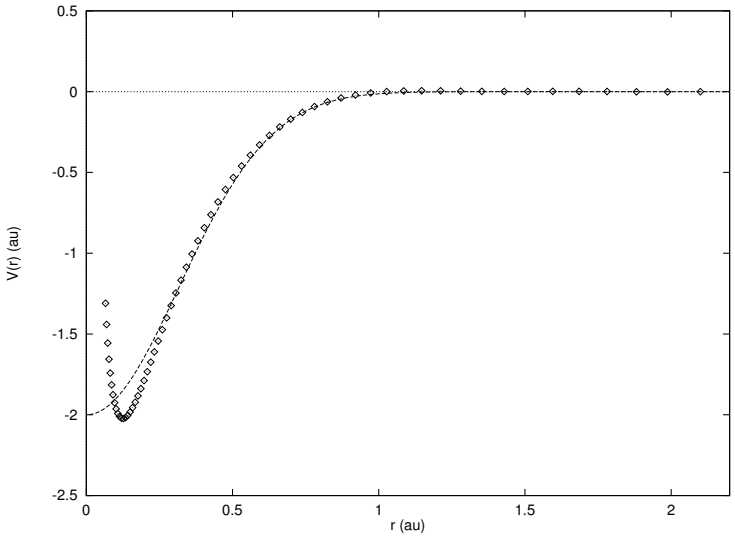

Figure 10: Gauss potential resulting from the inversion of eight phase shifts $l = 0, 1, ...7$ at $E_{cm} = 1.125$ a.u. ($k = 1.5$ a.u.).

The internal Hamiltonian has the eigenvalues $\varepsilon_{\nu J}$

$$\hat{h}(\xi)\chi_{\nu JM}(\xi) = \varepsilon_{\nu J}\chi_{\nu JM}(\xi).$$

where J is the total intrinsic angular momentum. The interaction potential is short-ranged up to $r \leq a$:

$$\hat{W}(\boldsymbol{r}, \xi) = \sum_{\lambda=0}^{\infty} \sum_{\mu=-\lambda}^{\lambda} Q_{\lambda\mu}(r, \xi) Y^*_{\lambda\mu}(\Omega).$$

The stationary solution of the coupled channel problem $\hat{H}\psi = E\psi$ can be written as

$$\Psi^I_M(\boldsymbol{r}, \xi) = \sum_{\nu J} \sum_{\ell=|I-J|}^{I+J} \left[i^\ell Y_\ell(\Omega) \otimes \chi_{\nu J}(\xi) \right]^I_M R^I_{\ell\nu J,n}(r)/r$$

where $\otimes$ denotes the tensor product of the spherical harmonics $Y_{\ell m}$ and the internal wave functions $\chi_{\nu JM}(\xi)$. In the following we use the coupled differential equations for the radial wave functions

$$\left(-\frac{\hbar^2}{2\mu}\frac{d^2}{dr^2} + \frac{\ell_\alpha(\ell_\alpha+1)\hbar^2}{2\mu r^2} + \varepsilon_\alpha - E \right) R^I_{\alpha n}(r) = -\sum_\beta \sum_\lambda C^{\lambda I}_{\alpha\beta} v^\lambda_{\nu_\alpha J_\alpha, \nu_\beta J_\beta}(r) R^I_{\beta n}(r).$$

Here, $\alpha = \{\ell_\alpha, \nu_\alpha, J_\alpha, \varepsilon_\alpha\}$ denotes the sets of quantum numbers of each channel, $C^{\lambda I}_{\alpha\beta}$ are coefficients depending on Clebsch-Gordan-coefficients and $3j-$Wigner-symbols and $v^\lambda_{\nu_\alpha J_\alpha, \nu_\beta J_\beta}(r)$ are reduced matrix elements of the coupling potentials $Q_\lambda(r, \xi)$.
We have constructed a possible solution of the inverse problem for coupled channels at fixed energy based on the Born approximation. For elastic scattering this method was developed by Ramm. The solution of the coupled differential equations from above

$$\left(\frac{d^2}{dr^2} - \frac{\ell_\alpha(\ell_\alpha+1)\hbar^2}{2\mu r^2} + k^2_\alpha \right) R^I_{\alpha n}(r) = \sum U^I_{\alpha\beta}(r) R^I_{\beta n}(r). \tag{9}$$

with $U^I_{\alpha\beta}(r) = \left(\frac{2\mu}{\hbar^2}\right) V^I_{\alpha\beta}(r)$, $k^2_\alpha = (E - \varepsilon_\alpha)\left(\frac{2\mu}{\hbar^2}\right)$, can be transformed to

$$R^I_{\alpha n}(r)/r = R^{0I}_{\alpha n}(r)/r$$

$$-i \int_0^a r'^2 dr' k_\alpha j_{\ell_\alpha}(k_\alpha r_<)(j_{\ell_\alpha}(k_\alpha r_>) + i n_{\ell_\alpha}(k_\alpha r_>)) \sum_\beta U^I_{\alpha\beta}(r') R^I_{\beta n}(r')/r',$$

where $R^{0I}_{\alpha n}(r)$ are regular solutions of

$$\left(\frac{d^2}{dr^2} - \frac{\ell_\alpha(\ell_\alpha+1)}{r^2} + k^2_\alpha\right) R^{0I}_{\alpha n}(r) = 0.$$

In the above equation (9) we assumed that the potential matrix vanishes for $r > a$. Then the above wave functions can be written for $r > a$:

$$R^I_{\alpha n}(r)/r = \sqrt{k_\alpha k_n}\delta^I_{\alpha n} j_{\ell_\alpha}(k_\alpha r) - i I^I_{\alpha n}(j_{\ell_\alpha}(k_\alpha r) + i n_{\ell_\alpha}(k_\alpha r)),$$

$$I^I_{\alpha n} = \int_0^a r'^2 dr' k_\alpha j_{\ell_\alpha}(k_\alpha r') \sum_\beta U^I_{\alpha\beta}(r') R^I_{\beta n}(r')/r'. \tag{10}$$

Comparison with the asymptotic wave function

$$R^I_{\alpha\beta}(r > a)/r = \frac{\sqrt{k_\alpha k_\beta}}{2}\left((S^I_{\alpha\beta} + \delta^I_{\alpha\beta}) j_{\ell_\alpha}(k_\alpha r) + i(S^I_{\alpha\beta} - \delta^I_{\alpha\beta}) n_{\ell_\alpha}(k_\alpha r)\right),$$

yields

$$S^I_{\alpha\beta} = \delta^I_{\alpha\beta} - \frac{2 i I^I_{\alpha\beta}}{\sqrt{k_\alpha k_\beta}}.$$

Up to here the formulas are exact expressions. Now we applied the first Born approximation by inserting the free solution $R^{0I}_{\beta n}(r)/r = \sqrt{k_\beta k_n}\delta^I_{\beta n} j_{\ell_\beta}(k_\beta r)$ instead of $R^I_{\beta n}(r)/r$ into the interaction matrix (10) and obtained:

$$\frac{I^I_{\alpha\beta}}{\sqrt{k_\alpha k_\beta}} \longrightarrow \tilde{I}^I_{\alpha\beta} = \sqrt{k_\alpha k_\beta} \int_0^a r'^2 dr' j_{\ell_\alpha}(k_\alpha r') U^I_{\alpha\beta}(r') j_{\ell_\beta}(k_\beta r').$$

The last relation leads to the basic equation for the inversion procedure:

$$S^I_{\alpha\beta} = \delta^I_{\alpha\beta} - 2 i \tilde{I}^I_{\alpha\beta}.$$

In order to get the potential matrix $U^I_{\alpha\beta}(r)$, one has to resolve the moments $b^\lambda_{\alpha\beta}$ of the transition matrix:

$$\int_0^a r'^2 dr' j_{\ell_\alpha}(k_\alpha r') j_{\ell_\beta}(k_\beta r') \langle \chi_{\nu_\alpha J_\alpha} || Q_\lambda(r', \xi) || \chi_{\nu_\beta J_\beta} \rangle = b^\lambda_{\alpha\beta},$$

where the $b^{\lambda}_{\alpha\beta}$ are given as a function of the S-matrix

$$b^{\lambda}_{\alpha\beta} = \frac{i\hbar^2\sqrt{4\pi}}{4\mu\sqrt{k_\alpha k_\beta}} i^{\ell_\alpha-\ell_\beta}(-1)^{J_\alpha+\lambda}\sqrt{\frac{2\lambda+1}{(2\ell_\alpha+1)(2\ell_\beta+1)}}\begin{pmatrix} \ell_\alpha & \lambda & \ell_\beta \\ 0 & 0 & 0 \end{pmatrix}^{-1}$$

$$\times \sum_I (-1)^I (2I+1)\begin{Bmatrix} J_\beta & \ell_\beta & I \\ \ell_\alpha & J_\alpha & \lambda \end{Bmatrix}(S^I_{\alpha\beta}-\delta^I_{\alpha\beta}).$$

The potential matrix can be obtained with the method of Backus and Gilbert. With $b^{\lambda}_{\alpha\beta} = b^{\lambda}_{i\ell_\alpha,j\ell_\beta}$ we introduced the ansatz

$$\langle i||Q_\lambda(r,\xi)||j\rangle_{I_{max}} = \sum_{\{\ell_\alpha,\ell_\beta\}=0}^{I_{max}} h^{\lambda}_{i\ell_\alpha,j\ell_\beta}(r) b^{\lambda}_{i\ell_\alpha,j\ell_\beta}$$

$$= \sum_{\{\ell_\alpha,\ell_\beta\}=0}^{I_{max}} h^{\lambda}_{i\ell_\alpha,j\ell_\beta}(r)\int_0^a r'^2 dr' j_{\ell_\alpha}(k_i r') j_{\ell_\beta}(k_j r')\langle i||Q_\lambda(r',\xi)||j\rangle.$$

This is fulfilled for $I_{max}\to\infty$ if

$$A^{\lambda,I_{max}}_{i,j}(r,r') = \sum_{\{\ell_\alpha,\ell_\beta\}=0}^{I_{max}} h^{\lambda}_{i\ell_\alpha,j\ell_\beta}(r) j_{\ell_\alpha}(k_i r') j_{\ell_\beta}(k_j r') r'^2 \to \delta(r-r').$$

From this equation we constructed linear inhomogeneous equations for the unknown functions $h^{\lambda}_{i\ell_\alpha,j\ell_\beta}(r)$ and then calculated the potential matrix.
Examples for testing this method were worked out by Jesgarz. Two intrinsic states were assumed with the same energies $\varepsilon_1=\varepsilon_2=0$ and angular momenta $J_1=J_2=0$. It follows $k_1=k_2=k$. Coupling potentials had $\lambda=0$ and $\hbar^2/\mu = 40$ MeV fm^2. For a first set of this inversion method we chose the coupling potential matrix in the form of a box potential

$$\boldsymbol{V}(r) = \begin{pmatrix} 100-50i & 10-i \\ 10-i & 50 \end{pmatrix}\text{ MeV} \quad \text{if} \quad r\le 1 \text{ fm}. \tag{11}$$

Further we took $k=5$ fm^{-1} and $I_{max}=8$. With these parameters and with $V=100$ MeV and $ka=5$ the condition of the first Born approximation yields $\mu V a^2/(\hbar^2 ka)=0.5$ which is on the border of the validity of the first Born approximation. As Fig. 11 shows, the inversion method also works for this special box coupling potential sufficiently well, reproducing the steps in the potential matrix $\boldsymbol{V}$ at $r=1$ fm.

3.6 Stability of static solitonic excitations of two-component Bose-Einstein condensates in finite range of interspecies scattering length

Over the past few years an increasing interest can be observed in the case of atomic Bose-Einstein condensates (BECs). Mostly one-component BECs have been studied so far for the elements ^{1}H, ^{7}Li, ^{23}Na, ^{41}K, ^{85,87}Rb, and ^{133}Cs. The two-component systems Na-Rb and K-Rb have been considered theoretically and the mixture Cs-Li has been

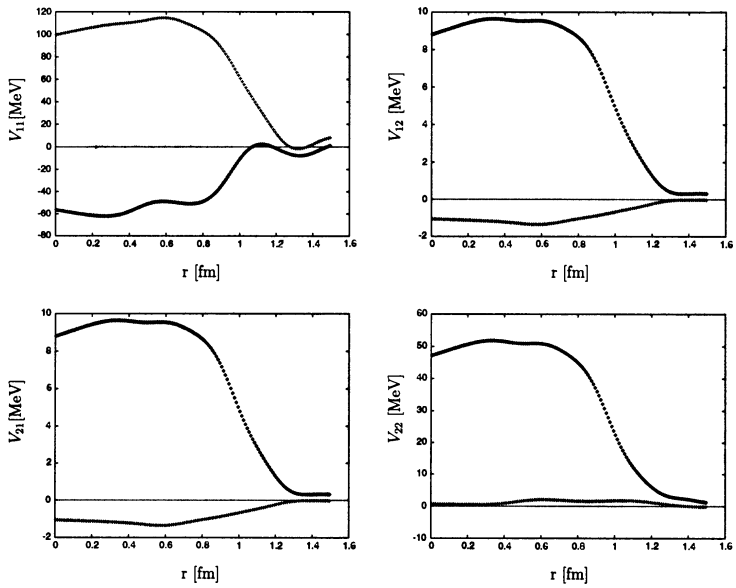

Figure 11: Inverted potential matrix calculated from the S-matrix obtained with $\boldsymbol{V}$ given in Eq. (11). The excitation energy is set to zero. The further parameters are $k = 5$ fm^{-1}, $a = 1.4$ fm and $I_{max} = 8$.

investigated experimentally, without reaching the BEC phase. In this project we give a simple treatment of the stability of a condensate mixture consisting of two atomic species (D. Schumayer, B. Apagyi, Phys. Rev. A **69** (2004) 043620).
For treating two interacting dilute Bose condensates we started with the zero temperature mean field theory neglecting collisions between the condensed atoms and the thermal cloud. The macroscopic dynamics in such a physical condensate is described by two coupled nonlinear Schrödinger equations (NLSs). These equations are also known as Gross-Pitaevskii (GP) equations. Restricting ourselves to $(1+1)$ dimensions the coupled GP equations can be written as follows $(i, j = 1, 2)$

$$i\hbar\frac{\partial\psi_i}{\partial t} = \left[-\frac{\hbar^2}{2m_i}\frac{\partial^2}{\partial x^2} + \sum_{j=1}^{2}\Omega_{ij}|\psi_j|^2 + V_i\right]\psi_i, \tag{12}$$

where m_i denotes the individual mass of the ith atomic species, $\Omega_{ij} = 2\pi\hbar^2 a_{ij}/A\mu_{ij}$ with a_{ij} being the 3-dimensional scattering length between atoms of species i, j, respectively, A the general transverse crossing area of the cigar-shape BEC, $\mu_{ij} = m_i m_j/(m_i + m_j)$ the reduced mass, and V_i, $(i = 1, 2)$ in Eq (12) are the external trapping potentials. The normalization of the wave functions is given by $N_i = \int_{-\infty}^{\infty}|\psi_i|^2 dx$, for $i = 1$ and 2 with N_i denoting the number of the individual atoms in the i^{th} component of the BEC.
The stationary solutions of the coupled GP equations (12) are taken in the form $\psi_i(x,t) = \Phi_i(x)\exp(-iE_i t/\hbar)$ where E_i is the single-particle energy of the i^{th} component. With this wave function and neglecting the kinetic terms in (12) we derived approximate density profiles and a semi-infinite range for the scattering length a_{ij} between two different atoms.

From the GP equations (12) we obtained the so called Thomas-Fermi approximation

$$|\Phi_1(x)|^2 = \frac{\Omega_{22}(E_1 - V_1(x)) - \Omega_{12}(E_2 - V_2(x))}{\Delta},$$

$$|\Phi_2(x)|^2 = \frac{\Omega_{22}(E_2 - V_2(x)) - \Omega_{21}(E_1 - V_1(x))}{\Delta}$$

with $\Delta = \Omega_{11}\Omega_{22} - \Omega_{12}\Omega_{21}$. With a harmonic external potential $V_i(x) = \frac{1}{2}m_i\omega_i^2 x^2 \quad (i = 1, 2)$ one can write $(i = 1, 2)$

$$\begin{aligned} |\Phi_i(x)|^2 &= A_i(x_i^2 - x^2)/\Delta \quad \text{if} \quad |x| \leq x_i, \quad i = 1, 2, \\ |\Phi_i(x)|^2 &= 0 \quad \text{if} \quad |x| > x_i, \quad i = 1, 2. \end{aligned}$$

The constants are $A_i = (\Omega_{jj}m_i\omega_i^2 - \Omega_{ij}m_j\omega_j^2)/2$ and $x_i = \pm(3\Delta N_i/4A_i)^{1/3}$ obtained from the normalization condition $\int_{-x_i}^{x_i} |\Phi_i(x)|^2 \mathrm{d}x = N_i$ $(i = 1, 2)$.
The excited static solutions have the form $(i = 1, 2)$

$$\tilde{\psi}_i(x, t) = \Phi_i(x)\phi_i(x) \exp(-i\tilde{E}_i t/\hbar)$$

with $\phi_i(x)$ being an excess or defect of the i^{th} component of the background density. Inserting this ansatz into the GP equations (12) and assuming that the excitation mechanism is restricted to a small interval $x \in (-L_i, L_i)$ around $x = 0$, one obtains two coupled equations for the perturbing functions

$$\tilde{E}_1\phi_1 = -\frac{\hbar^2}{2m_1}\frac{\partial^2\phi_1}{\partial x^2} + \tilde{\Omega}_{11}|\phi_1|^2\phi_1 + \tilde{\Omega}_{12}|\phi_2|^2\phi_1 \tag{13a}$$

$$\tilde{E}_2\phi_2 = -\frac{\hbar^2}{2m_2}\frac{\partial^2\phi_2}{\partial x^2} + \tilde{\Omega}_{21}|\phi_1|^2\phi_2 + \tilde{\Omega}_{22}|\phi_2|^2\phi_2 \tag{13b}$$

with $\tilde{\Omega}_{ij} = \Omega_{ij}A_j x_j^2/\Delta$ $(i, j = 1, 2)$. Very small potential terms have been neglected. These equations determine the perturbing functions $\phi_i(x)$ within the range $|x| \leq L_i < x_i$. Since static one-soliton solution of the B or the D type can be produced in BECs we tried to use static uncoupled soliton solutions

$$\phi_{B1}(x) = q_1 \mathrm{sech}(k_1 x)$$

$$\phi_{D2}(x) = q_2 \tanh(k_2 x)$$

with complex amplitudes q_i and range parameters $k_i \sim L_i^{-1}$ for the description of the excitation of the two-component BECs. In accordance with the soliton characters we impose the appropriate boundary conditions $\phi_{B1}(x \to \pm\infty) = 0$, and $\phi_{D2}(x \to \pm\infty) = \pm q_2$.
The insertion of the above solitonic ansatz into equations (13) gives $k_1 = k_2 \equiv k$ for the range parameters and the relations

$$|q_1|^2 = \frac{\hbar^2 k^2}{\Delta}\left(\frac{\tilde{\Omega}_{12}}{m_2} - \frac{\tilde{\Omega}_{22}}{m_1}\right),$$

$$|q_2|^2 = \frac{\hbar^2 k^2}{\Delta}\left(\frac{\tilde{\Omega}_{11}}{m_2} - \frac{\tilde{\Omega}_{21}}{m_1}\right)$$

for the modulus of the amplitudes.
The requirement that the modulus of the two amplitudes q_1 and q_2 is positive and real yields the stability conditions $(A_{ij} = a_{ij}(1 + m_i/m_j))$

$$f_{B1}(a_{12}) = \frac{A_{12} - A_{22}}{\det(A)} \geq 0, \tag{14a}$$

$$f_{D2}(a_{12}) = \frac{A_{11} - A_{21}}{\det(A)} \geq 0 \tag{14b}$$

for the existence of B and D solitonic excitation within the two component BEC. Although the above conditions are independent of the particle numbers N_i, one has a constraint by the particle number conservation because the normalization of the B and D solitonic excitation reads as

$$N_1 = 2|q_1|^2 \frac{A_1}{\Delta} n(kx_1),$$

$$N_2 = 2|q_2|^2 \frac{A_2}{\Delta}\left(\frac{2}{3}(kx_2)^2 - n(kx_2)\right),$$

with $n(w) = -w^2 + 2w\ln[1 + exp(2w)] + \mathrm{dilog}[1 + exp(2w)] + \frac{\pi^2}{12}$.
Assuming now that the system parameters m_1, m_2, a_{11} and a_{22} are given, and disregarding the particle numbers N_i, one can determine the broadest range of the interspecies scattering length a_{12} for which the existence of solitons in the two-component BEC can be expected. If the actual value of a_{12} is determined then one can find the particle number ratio N_2/N_1 or the size parameter k in order to get information about the two-component system which may show static solitonic features.
In Fig.12 we show the density profile $|\Phi_i|^2$ of the Thomas-Fermi approximation for a two-component BEC, namely for the mixture ^{7}Li - ^{87}Rb, with parameters $a_{11} = -1.4$ nm (^{7}Li), $a_{22} = 5.5$ nm (^{87}Rb) and the chosen interspecies scattering length $a_{12} = 4.5$ nm.

3.7 Assessment of interspecies scattering lengths a_{12} from stability of two-component Bose-Einstein condensates

Tables 1 and 2 give, separated from each other by semicolons, the limiting point values of the intervals of the interspecies scattering length a_{12} satisfying the stability conditions encoded into inequalities (14a-b). These conditions express the possibility of developing solitonic excitations of static BD or DB type from the ground state of the two-component BECs, irrespective of the particle numbers N_1 and N_2 of the mixture. The data have been calculated, respectively, with triplet and singlet intraspecies scattering lengths a_{ii} $(i = 1, 2)$ listed in the columns headed by the labels a_t and a_s. The exception is the ^{133}Cs atom where only the average scattering length $(a_{ii} = +\sqrt{\sigma_{exp}/8\pi})$ has been available (therefore the parenthesis).
In general we observe in tables 1 and 2 that one of the limiting points of the intervals of the corresponding DB and BD cases coincides; a fact easily derivable by using the

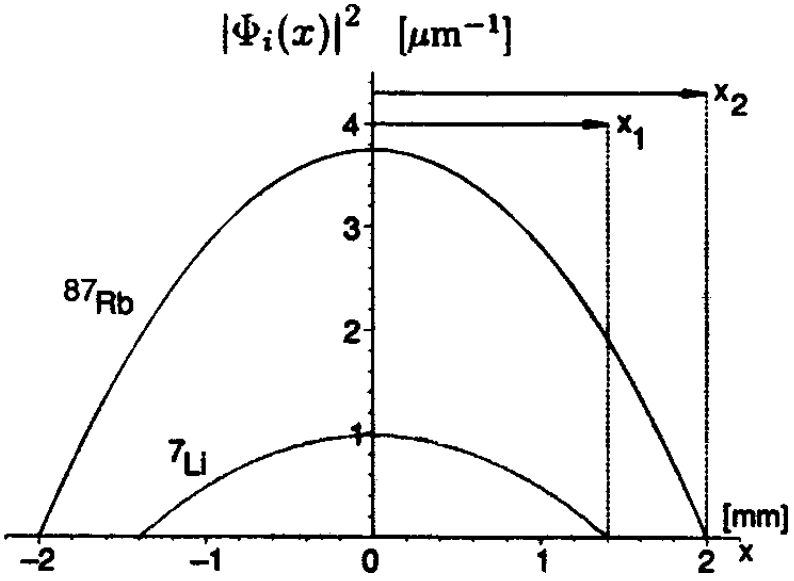

Figure 12: The density profile $|\Phi_i|^2$ of the Thomas-Fermi approximation for a two-component BEC, namely for the mixture ^{7}Li - ^{87}Rb, with parameters $a_{11} = -1.4$ nm (^{7}Li), $a_{22} = 5.5$ nm (^{87}Rb) and $a_{12} = 4.5$ nm.

relation $0 = f_{B1}(a_{12}) = f_{D2}(a_{12})$. The diagonal elements of tables 1 and 2 represent one-component BECs which is out of scope of the present interest so that the data are missing there. Furthermore, the rows corresponding to ^{7}Li, ^{39}K, and ^{85}Rb of table 1 do not contain any results as well, if their partner owns a positive triplet intraspecies scattering length. The lack of information means here that we do not find any region of triplet interspecies scattering length a_{12} which gives rise to a stable DB type excitation. On the other hand all items of the column headed by ^{7}Li, ^{39}K, and ^{85}Rb are filled by data. This means that there are definite ranges of triplet a_{12} which support BECs with excitations of BD type where the ^{7}Li, ^{39}K, and ^{85}Rb atoms play the role of the B component (owing to their attractive interaction character). The above argumentation can be confirmed by using stability conditions (14a-b) with $a_{11} < 0$ and $a_{22} > 0$.

In the case when both a_{11} and a_{22} are positive we observe the existence of BECs with both DB or BD formations within a finite interval of positive interspecies scattering length a_{12}. This can be understood physically in the following way. In the context of the mean field theory, an effective potential is created by the i-th atoms acting repulsively among each other (positive scattering lengths) and thus forming the cavity of the D component. Inside this cavity there is a possibility for the j-th atoms to form a bunch representing the B component despite their inherent repulsive character.

The values of a_{12} given in tables 1 and 2 can be used for orientation and in design of two-component BECs. One starts from known intraspecies scattering lengths a_{ii} ($i = 1, 2$) which are represented by the data denoted by a_t or a_s in the tables. Then one performs the range determination by using inequalities (14a-b). Now one is provided with guessed values of interspecies scattering length a_{12} which can maintain stable two-component BEC configuration. If, from some other sources, we are assured that the actual physical

values of a_{12} falls outside the range calculated then one may try either to move the a_{ij} values into the proper direction by utilizing the Feshbach-resonance procedure or to carry out BB or DD stability analyses to learn what type (if any) of static solitonic excitations of the components are possible (suggesting, at the same time, stability of the ground state configurations as well).

3.8 Evolution solution (simulation) of the nonlinear Schrödinger equation

Our aim is to solve the evolution problem of the Gross-Pitaevskii (GP) equation

$$iu_t = -HV\, u_{xx} + C\,|u|^2 u + Vu, \quad u = u(x,t), \quad V = V(x) \tag{15}$$

with given initial condition $u_0(x) = u(x,0)$. In the case of special values of the constants HV and C, and for zero potential $V = 0$ there are some exact solutions to the remaning equation known also as the nonlinear Schrödinger (nls) equation.

$$iu_t = -HV\, u_{xx} + C\,|u|^2 u, \quad u = u(x,t). \tag{15a}$$

Colliding two-soliton solution

Let us consider the following nls equation

$$iu_t = u_{xx} + 2|u|^2 u \tag{16}$$

which means that we use $HV = -1, C = +2$ and $V = 0$ in (15).
Equation (16) admits the following (colliding) two-soliton solution:

$$u(x,t) = \frac{e^{-i(2x-20-3t)}}{\cosh(x-10-4t)} + \frac{e^{+i(2x+20-3t)}}{\cosh(x+10+4t)} \tag{17}$$

Bright soliton solution

The most widely known soliton solution of the nls equation of the form

$$iu_t = -u_{xx} - |u|^2 u \qquad (HV = 1, C = -1, V = 0) \tag{18}$$

is the bright soliton. Its general form is the following:

$$u(x,t;a,c) = a\, e^{i(\frac{c}{2}(x-ct)+nt)} / \cosh(a(x-ct)/\sqrt{2}) \tag{19}$$

with the constraint that $a^2 = 2(n - \left(\frac{c}{2}\right)^2) > 0$.
If $c = 1$, $n > \frac{1}{4}$. Let $n = \frac{5}{4}$. Then $a^2 = 2$, $a = \sqrt{2}$. The bright soliton solution is then

$$u(x,t;\sqrt{2},1) = \sqrt{2} e^{i(\frac{1}{2}(x-t)+\frac{5}{4}t)} / \cosh(x-t). \tag{20}$$

The initial condition in this case is

$$u(x,0;\sqrt{2},1) = \sqrt{2} e^{ix/2} / \cosh(x) \tag{21a}$$

and the norm is (independent of t):

$$\int |u(x,t;\sqrt{2},1)|^2 \mathrm{d}x = 4. \tag{21b}$$

In case of $c = 2$ we have the bright soliton

$$u(x,t;\pm 2,2) = \pm 2e^{i((x-2t)+3t)}/\cosh(\pm\sqrt{2}(x-2t)), \tag{22}$$

and the initial condition

$$u(x,0;\pm 2,2) = \pm 2e^{ix}/\cosh(\pm\sqrt{2}x). \tag{22a}$$

Dark soliton solution
The nls equation

$$iu_t = -u_{xx} + |u|^2 u \qquad (HV = 1, C = +1, V = 0) \tag{23}$$

supports dark soliton solution of the form

$$u(x,t;m,c) = re^{i(\Theta - mt)}, \tag{23a}$$

with real amplitude $r = r(x-ct)$, real phase $\Theta = \Theta(x-ct)$, and real parameters $c = const$, $m = const > c^2/2 > 0$ satisfying the relations

$$r^2 = m - 2\kappa^2/\cosh^2(\kappa(x-ct))$$

and

$$1/\tan(\Theta) = -2\kappa\tanh(\kappa(x-ct)).$$

In the course of testing the simulation program we shall use the dark soliton solution with parameters $m = 1, c = 1$.
Ma solitary wave solution
Equation

$$iu_t = -u_{xx} - |u|^2 u \qquad (HV = 1, C = -1, V = 0) \tag{24}$$

also has the Ma solitary wave solution of the form

$$u(x,t;a,m) = ae^{ia^2 t}[1 + 2m(m\cos\Theta + in\sin\Theta)/f(x,t)] \tag{25}$$

with real parameters a and m and the following relations and definitions:

$$n^2 = 1 + m^2, \quad \Theta = 2mna^2 t, \quad f(x,t) = n\cosh(ma\sqrt{2}x) + \cos\Theta.$$

In the course of testing the simulation program we shall use the Ma solitary wave solution with parameters $a = 1, m = 1/2$.
Rational-cum-oscillatory solution
Equation

$$iu_t = -u_{xx} - |u|^2 u \qquad (HV = 1, C = -1, V = 0) \tag{26}$$

also has the rational-cum-oscillatory solution of the form

$$u(x,t) = e^{it}\left[1 - \frac{4(1+2it)}{1+2x^2+4t^2}\right] \tag{27}$$

Simulation procedure

To solve the time evolution problem of the Schrödinger equation

$$iu_t(x,t) = Hu(x,t), \quad u(x,t) = e^{-iHt}u(x,t) \tag{28}$$

one discretises eq. (28) in time, $t_n = n\tau$ ($n = 0, 1, .., NT$), and space, $x_j = jh$ ($j = 1, 2, ..., N$), and denotes the wave function by $u_j^n \equiv u(x_j, t_n)$.
One makes use of the basic relation that the backward and forward time evolutions at $t_{n+1/2}$ result in the same value of the wave function at every point x_j, that is

$$u_j^{n+1/2} = (1 + \frac{1}{2}iH\tau)u_j^{n+1} = (1 - \frac{1}{2}iH\tau)u_j^n = u_j^{n+1/2} \tag{29}$$

or, using instead of $1/2$ the symbol σ,

$$u_j^{n+\sigma} = (1 + \sigma iH\tau)u_j^{n+1} = (1 - \sigma iH\tau)u_j^n = u_j^{n+\sigma}, \tag{29a}$$

We obtain the backward evolution at $\sigma = 0$, the forward evolution at $\sigma = 1$. The Cranck-Nicholson scheme corresponds to $\sigma = 1/2$.
By re-ordering equation (29a) one gets the basic formula:

$$iu_j^{n+1} - \tau H\sigma u_j^{n+1} = iu_j^n + \tau(1-\sigma)Hu_j^n \tag{30}$$

with the Hamiltonian acting at point x_j on the wave funcion u_j as

$$Hu_j = -\frac{HV}{h^2}(u_{j+1} - 2u_j + u_{j-1}) + V_j u_j$$

with $V_j = V(x_j) + C|u_j|^2$. By using this form, eq.(30) can be written into a form

$$T^{(n)}u^{n+1} = F^n \tag{31}$$

where $T^{(n)}$ denots an NxN triangular matrix with elements $T_{j,j}^{(n)} = B_j^{(n)} = ih^2 - \tau\sigma(2HV + h^2V_j)$, $T_{j+1,j}^{(n)} = T_{j,j+1}^{(n)} = A = \tau\sigma HV$ and F^n stands for an $1xN$ vector whose elements are defined by $F_j^n = C_j^n u_j^n - D(u_{j+1}^n + u_{j-1}^n)$ with $C_j^{(n)} = ih^2 + \tau(1 - \sigma)(2HV + h^2V_j)$ and $D = \tau(1-\sigma)HV$.
We use Neumann boundary condition $u_x = 0$ at the boundaries. At the boundary the formula (30) provides the relation

$$u_j^{n+1} = \frac{i + \tau(1-\sigma)V_j}{i - \tau(1-\sigma)V_j}u_j^n, \quad i = 1, N \tag{32}$$

Outraying
By starting with $y(x, 0)$ which does not correspond to an exact solution the 'rest' is is outraying and only the stable soliton configuration remains.

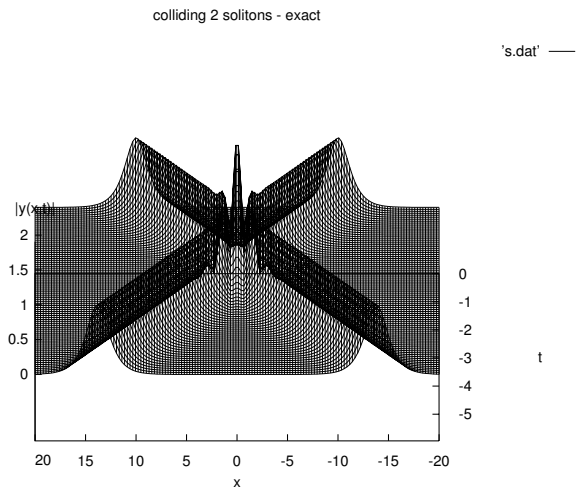

Figure 13: Coliding solitons - exact case (see eq.(17)).

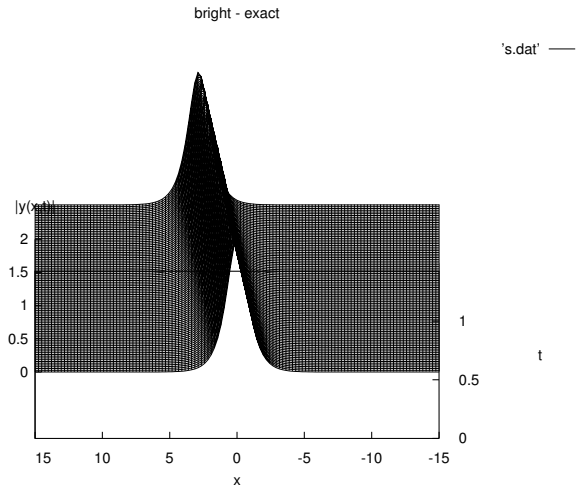

Figure 14: Brigth soliton - exact case (see eq.(19)).

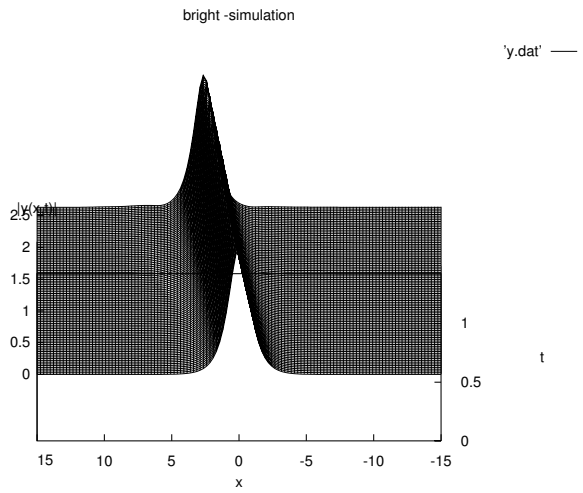

Figure 15: Brigth soliton - simulation (see eq.(31)).

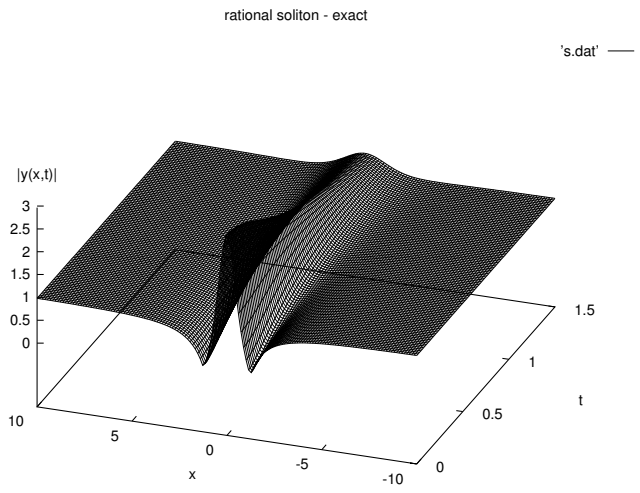

Figure 16: Brigth soliton - exact case (see eq.(22)).

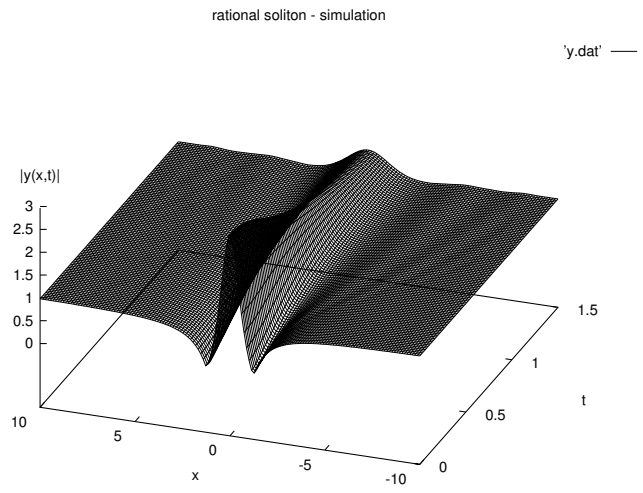

Figure 17: Brigth soliton - simulation (see eq.(31)).

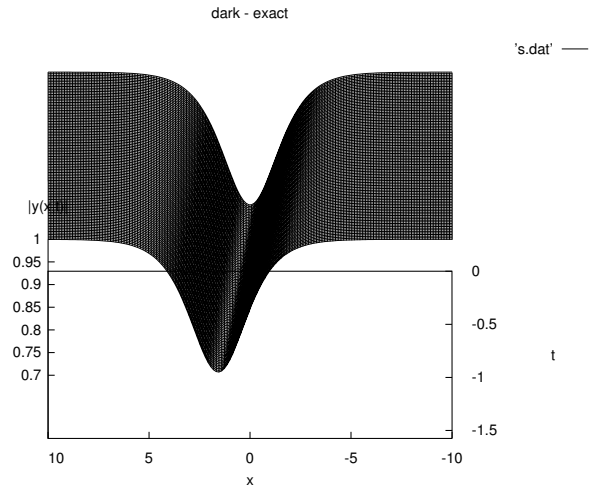

Figure 18: Dark soliton - exact case (see eq.(23a)).

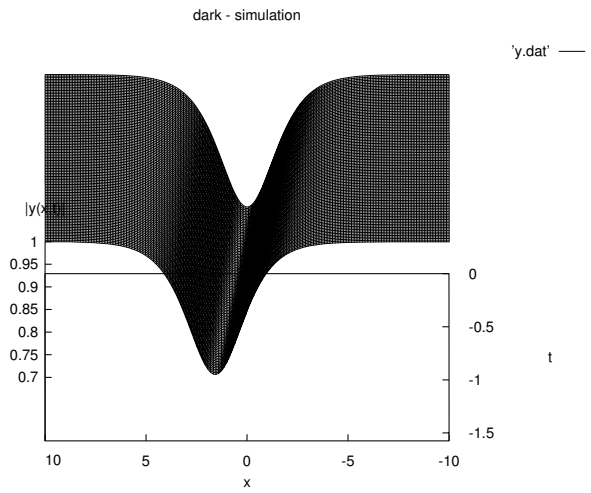

Figure 19: Dark soliton - simulation (see eq.(31)).

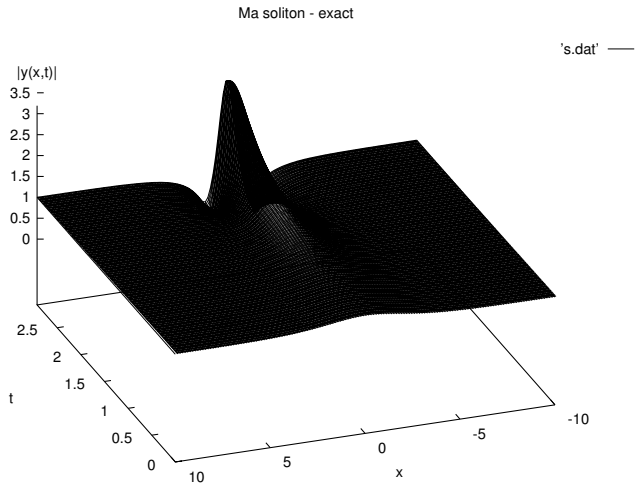

Figure 20: Ma solitary wave - exact case (see eq.(25)).

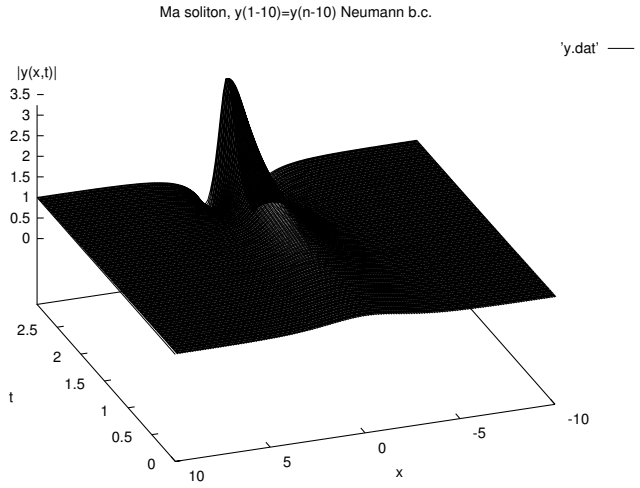

Figure 21: Ma solitary wave - simulation. Neumann b.c. used at j=1-10 and N-10 - N. (see eq.(32)).

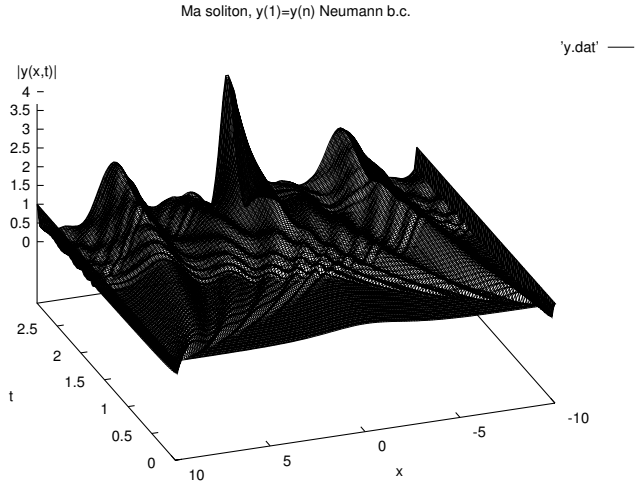

Figure 22: Ma solitary wave - simulation. Neumann b.c. used at j=1 and N. (see eq.(32)).

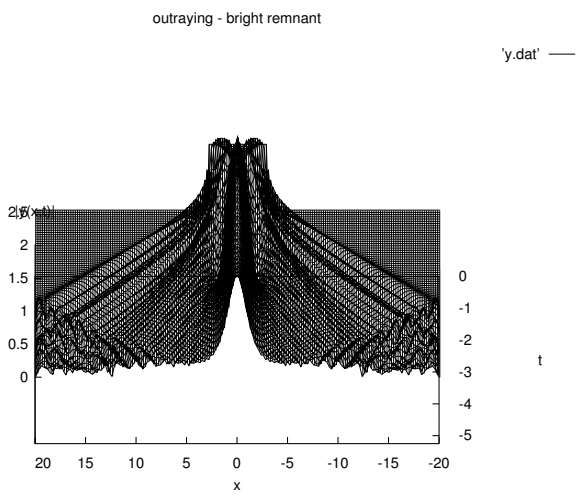

Figure 23: By starting with $y(x,0)$ which does not correspond to an exact solution the 'rest' is is outraying and only the stable soliton configuration remains. Here one soliton.

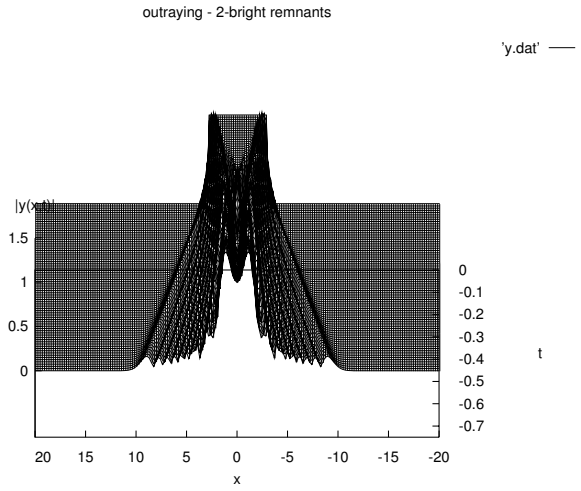

Figure 24: By starting with $y(x,0)$ which does not correspond to an exact solution the 'rest' is is outraying and only the stable soliton configuration remains. Here two solitons.

Table 1: Intervals of triplet interspecies scattering lengths a_{12} assessed by static solitonic excitations of two component BECs composed of alkalis indicated. The column $a_{\rm t}$ gives the triplet intraspecies scattering length a_{ii} taken from the references. All values are in unit of nm.

			Bright-component									
	Element	$a_{\rm t}$	^{1}H	^{7}Li	^{23}Na	^{39}K	^{41}K	^{83}Rb	^{85}Rb	^{87}Rb	^{133}Cs	^{135}Cs
Dark-component	^{1}**H**	0.1		-2.4;0.0	0.0;0.2	-1.8;0.0	0.0;0.2	0.0;0.1	-37.6;0.0	0.0;0.2	0.0;0.1	0.0;0.1
	^{7}**Li**	−1.4	–;–		–;–	-1.5;-0.8	–;–	–;–	-35.1;-2.7	–;–	–;–	–;–
	^{23}**Na**	4.0	0.2;7.7	-0.6;6.1		-1.1;3.0	2.8;3.5	1.7;3.4	-30;1.7	1.7;3.8	1.2;2.2	1.2;3.8
	^{39}**K**	−0.9	-0.4;-0.1	–;–	–;–		–;–	–;–	-26;-3.8	–;–	–;–	–;–
	^{41}**K**	3.4	0.1;6.6	-0.4;5.8	3.5;4.4	-0.9;3.5		2.3;3.6	-25.4;2.2	2.2;4.0	1.6;2.4	1.6;4.2
	^{83}**Rb**	4.2	0.1;8.3	-0.2;7.7	3.4;6.6	-0.6;5.7	3.6;5.6		-19.2;4.1	4.1;4.8	3.1;3.2	3.2;5.3
	^{85}**Rb**	−19.0	–;–	-2.7;-0.2	–;–	-3.8;-0.6	–;–	–;–		–;–	–;–	–;–
	^{87}**Rb**	5.5	0.2;10.9	-0.2;10.2	3.8;8.7	-0.6;7.6	4.1;7.5	4.8;5.6	-18.8;5.6		3.6;4.4	4.3;6.1
	^{133}**Cs**	(2.4)	0.0;4.8	-0.1;4.6	2.2;4.1	-0.4;3.7	2.4;3.7	3.0;3.1	-14.8;2.9	2.9;3.6		2.4;4.2
	^{135}**Cs**	7.2	0.1;14.3	-0.1;13.7	3.8;12.3	-0.4;11.2	4.2;11.1	5.3;8.9	-14.7;8.9	6.1;8.8	4.2;7.3	

Table 2: Intervals of singlet interspecies scattering lengths a_{12} assessed by static solitonic excitations of two component BECs composed of alkali pairs indicated. The column $a_{\rm S}$ gives the singlet scattering length a_{ii} of atoms taken from the references. (For ^{1}H the triplet value has been used). All values are in unit of nm.

			Bright-component									
	Element	$a_{\rm S}$	^{1}H	^{7}Li	^{23}Na	^{39}K	^{41}K	^{83}Rb	^{85}Rb	^{87}Rb	^{133}Cs	^{135}Cs
Dark-component	^{1}**H**	(0.1)		-0.0;0.2	0.0;0.2	0.0;0.2	0.0;0.2	0.0;0.1	0.0;0.6	0.0;0.1	0.0;0.1	0.0;0.2
	^{7}**Li**	1.7	0.2;3.0		0.8;1.8	0.5;2.5	0.5;1.6	0.3;1.3	0.3;7.7	0.3;1.5	0.2;0.9	0.2;2.9
	^{23}**Na**	2.7	0.2;5.3	1.8;4.2		2.0;4.3	1.9;3.3	1.2;2.5	1.2;15.1	1.1;2.9	0.8;1.8	0.8;6.0
	^{39}**K**	7.3	0.2;14.2	2.5;12.4	4.3;9.2		5.7;7.0	4.6;4.7	4.6;28.0	4.5;5.4	3.3;3.5	3.3;11.5
	^{41}**K**	4.4	0.2;8.6	1.2;5.4	3.3;5.7	4.6;5.7		3.0;3.7	2.9;22.1	2.9;4.3	2.1;2.8	2.0;9.0
	^{83}**Rb**	3.4	0.1;6.8	1.3;6.3	2.5;5.4	4.6;4.7	3.7;4.6		3.4;20.7	3.3;4.0	2.6;2.8	2.6;9.2
	^{85}**Rb**	124.8	0.6;246	7.7;230	15.1;196	28.0;171	22.1;167	20.7;126		24.2;123	16.9;97	55.5;96
	^{87}**Rb**	4.7	0.1;9.2	1.5;8.7	2.9;7.4	5.4;6.5	4.3;6.3	4.0;4.8	4.7;24.2		3.3;3.8	3.7;10.8
	^{133}**Cs**	(2.4)	0.1;4.8	0.9;4.6	1.8;4.0	3.5;3.7	2.8;3.7	2.8;3.0	3.0;16.9	2.9;3.3		2.7;7.9
	^{135}**Cs**	26.0	0.2;51.6	2.9;49.5	6.0;44.4	11.5;40.3	12.1;39.9	9.1;32.3	32.0;55.5	10.8;31.6	7.9;26.2	